Three-dimensional spin–orbit coupling in a trap

2013 J. Phys. B: At. Mol. Opt. Phys. 46 134003

(http://iopscience.iop.org/0953-4075/46/13/134003)

J. Phys. B: At. Mol. Opt. Phys. **46** (2013) 134003 (12pp) doi:10.1088/0953-4075/46/13/134003

Three-dimensional spin–orbit coupling in a trap

Brandon M Anderson and Charles W Clark

Joint Quantum Institute, National Institute of Standards and Technology and the University of Maryland, Gaithersburg, MD, 20899-8410, USA

E-mail: brandona@umd.edu

Received 14 December 2012, in final form 20 February 2013
Published 24 June 2013
Online at stacks.iop.org/JPhysB/46/134003

Abstract
We investigate the properties of an atom under the influence of a synthetic three-dimensional spin–orbit coupling (Weyl coupling) in the presence of a harmonic trap. The conservation of total angular momentum provides a numerically efficient scheme for finding the spectrum and eigenfunctions of the system. We show that at large spin–orbit coupling the system undergoes dimensional reduction from three to one dimension at low energies, and the spectrum is approximately Landau level-like. At high energies, the spectrum is approximately given by the three-dimensional isotropic harmonic oscillator. We explore the properties of the ground state in both position and momentum space. We find the ground state has spin textures with oscillations set by the spin–orbit length scale.

(Some figures may appear in colour only in the online journal)

1. Introduction

The recent experimental success in simulating spin–orbit coupling [1–5] in a cold atom context has produced great interest in the field. Although the experimental setup produced only an Abelian spin–orbit coupling, it is possible to produce more complicated non-Abelian synthetic fields, such as any combination of Rashba and linear Dresselhaus couplings [6–11]. The isotropic limit, such as Rashba or linear Dresselhaus coupling, is particularly interesting. In this limit, and the absence of an external potential, the spin–orbit coupling leads to an infinitely degenerate ground state manifold, which is given by a ring in momentum space. The ring of minima gives an energetically weak direction for low-energy quantum fluctuations. This leads to an effective dimensional reduction for low energy properties [12–14], such as a Landau-like spectrum [12, 14–16], enhanced binding energy [17–25], or spontaneous symmetry breaking [26]. In the presence of a trap or interactions this degeneracy will be broken, up to the two-fold degeneracy guaranteed by time-reversal symmetry. However, as we show here, effects of the infinite manifold of states will survive even to the trapped regime, and the dimensional reduction of low energy states will still be visible.

A recent proposal [16, 27, 28] allows for the study of spin–orbit coupling that has no solid state counterpart: three-dimensional (3D) spin–orbit coupling, or Weyl coupling [29], of the form: $v\mathbf{p}\cdot\boldsymbol{\sigma}$, where $\mathbf{p}$ is momentum, and $\boldsymbol{\sigma}$ is the spin operator. The conceptual picture in this system is similar to that of the Rashba case. However, instead of a ring of ground states we now have a spherical manifold of ground states. This implies there are two energetically weak directions for low energy quantum fluctuations, so the dimensional reduction is now from $D = 3$ to $D = 1$.

In this paper we analyse the motion of a particle moving in an isotropic harmonic trap, subject to Weyl coupling. We show that while Weyl coupling is the natural extension of Rashba coupling to incorporate the third spatial dimension, this extension actually increases the overall symmetry of the system and simplifies its treatment. We describe a numerical scheme for finding the eigenvalues exactly, and we analyse the eigenfunctions. Even the ground state of this system exhibits significant spin and orbital textures. In the limit of large coupling we find Landau-like behaviour of the spectrum, in that the low-energy spectrum tends to that of a one-dimensional harmonic oscillator with a large number of nearly degenerate levels. However, at sufficiently large energies, the spin–orbit coupling becomes a perturbation, and the high energy spectrum is well approximated by the 3D isotropic harmonic oscillator.

The paper is organized as follows. We first review the model Weyl coupling Hamiltonian. We perform a partial wave expansion of the system in the presence of a trap,

and find a numerically efficient method for diagonalizing the system. We calculate the spectrum as a function of the spin–orbit coupling strength, and find the low energy spectrum becomes Landau-like at large coupling. At sufficiently high energies, the spectrum crosses over to that of the 3D isotropic harmonic oscillator. We derive a system of coupled differential equations in the radial coordinate only, and use it to explain the crossover between the Landau spectrum and isotropic oscillator spectrum. Finally, we show the ground state is characterized by persistent orbital and spin currents.

2. Model

Our Hamiltonian is given by

$$H = \frac{\mathbf{p}^2}{2} + v\mathbf{p}\cdot\boldsymbol{\sigma} + \frac{\mathbf{r}^2}{2}, \tag{1}$$

where $\mathbf{r}$ and $\mathbf{p}$ are respectively the position and momentum operators and $\boldsymbol{\sigma} = (\sigma_1, \sigma_2, \sigma_3)$ is the vector of conventional Pauli matrices. This Hamiltonian can be implemented in cold atomic systems using two-photon transitions as described in [27]: here v is a coupling constant subject to external control. The two dimensions of the spin operator $\boldsymbol{\sigma}$ correspond to two dressed states of the atom, which would ordinarily be composed of many internal hyperfine states [9]. We have chosen a system of units in which the reduced Planck constant $\hbar$, the mass M of the particle, and the harmonic oscillator frequency ω are all equal to 1.

Our Hamiltonian commutes with an angular momentum $\mathbf{J} = \mathbf{L} + \frac{\sigma}{2}$, where $\mathbf{L} = \mathbf{r}\times\mathbf{p}$ is the orbital angular momentum of the atomic centre of mass. Note that this $\mathbf{J}$ need not be identical to the usual angular momentum that is constructed from the sum of the orbital angular momentum of the atom's centre of mass and the angular momenta of its electrons and nuclei. However, it is a conserved quantity whose three spatial components satisfy the usual commutation relations of an angular momentum operator, and in this sense we can treat $\mathbf{J}$ as the sum of an integer-valued orbital angular momentum $\mathbf{L}$ and a spin $s = \frac{1}{2}$. The $\boldsymbol{\sigma}\cdot\mathbf{p}$ term is a scalar under the rotations induced by $\mathbf{J}$, as is the kinetic and trapping term, so our Hamiltonian commutes with $\mathbf{J}$. We note in passing that Rashba coupling is obtained from removing the $\sigma_3 p_3$ term from Weyl coupling. Thus Rashba coupling is a linear combination of scalar and rank-2 tensor operators under rotations, whereas Weyl coupling has the simpler scalar form and is much simpler to solve with a standard partial-wave decomposition.

In the absence of a trap, the spectrum of the Weyl coupling can be found exactly. There are two bands corresponding to spin aligned, and anti-aligned with momentum. The spectrum is given by

$$E(\mathbf{p}) = \frac{\mathbf{p}^2}{2} \pm v|\mathbf{p}|. \tag{2}$$

The low energy band has a minimum defined on the sphere $|\mathbf{p}| = v$. Near the minimum of this sphere, the dispersion is parabolic only along the radial direction, and is quartic along the polar and azimuthal directions. This suggests that for low energy properties of the system, quantum fluctuations will be energetic primarily along the radial direction, with only a weak splitting due to angular fluctuations. We expect that in the presence of a spherically symmetric trap, the low energy spectrum of the system will undergo a dimensional reduction from $D = 3$ to $D = 1$ for a sufficiently large spin–orbit coupling.

The conserved total angular momentum $\mathbf{J}$ allows us to use a basis of well defined angular momentum $|j, m, \lambda\rangle$, where

$$|j, m, \lambda\rangle = \mathrm{e}^{\mathrm{i}\phi_\lambda}\begin{pmatrix} \lambda\sqrt{\dfrac{j - \lambda m + \frac{1+\lambda}{2}}{2\left(j + \frac{1+\lambda}{2}\right)}}\left|j + \dfrac{\lambda}{2}, m - \dfrac{1}{2}\right\rangle \\ -\sqrt{\dfrac{j + \lambda m + \frac{1+\lambda}{2}}{2\left(j + \frac{1+\lambda}{2}\right)}}\left|j + \dfrac{\lambda}{2}, m + \dfrac{1}{2}\right\rangle \end{pmatrix} \tag{3}$$

and $\lambda = \pm 1$ corresponds to $\mathbf{J}$ and $\boldsymbol{\sigma}$ aligned ($j = l + s$) or anti-aligned ($j = l - s$). These states have eigenvalues $\mathbf{J}^2|j, m, \lambda\rangle = j(j+1)|j, m, \lambda\rangle$ and $J_z|j, m, \lambda\rangle = m|j, m, \lambda\rangle$. They are complete, which allows us to project our Hamiltonian into subspaces of fixed j, m.

2.1. Number basis

The Weyl coupling Hamiltonian can be numerically diagonalized by performing a partial wave decomposition into states of the 3D isotropic harmonic oscillator, with angular momentum state $|j, m, \lambda\rangle$. We define the basis $|n, j, m, \lambda\rangle = |n\rangle\,|j, m, \lambda\rangle$ in appendix A as a state with n radial quantum nodes, and an angular momentum eigenstate given by (3). When $v = 0$ these states have energy $E = 2n + l + \frac{3+\lambda}{2}$ [30]. The spin–orbit coupling can be decomposed as

$$\mathbf{p}\cdot\boldsymbol{\sigma} = \frac{-\mathrm{i}}{\sqrt{2}}(\mathcal{A}^+ - \mathcal{A}^-) \tag{4}$$

where $\mathcal{A}^+ = \boldsymbol{\sigma}\cdot\mathbf{a}^\dagger$ and $\mathcal{A}^- = \boldsymbol{\sigma}\cdot\mathbf{a}$ are rank-0 tensors with respect to rotations generated by $\mathbf{J}$. The vectors $\mathbf{a}^\dagger = \left(a_x^\dagger, a_y^\dagger, a_z^\dagger\right)$ and $\mathbf{a} = (a_x, a_y, a_z)$ are respectively vectors of creation and annihilation operators, with $[a_i, a_j^\dagger] = \delta_{ij}$ and $[a_i, a_j] = [a_i^\dagger, a_j^\dagger] = 0$. The anti-commutation relation $\frac{1}{2}\{\mathcal{A}^+, \mathcal{A}^-\} = \mathbf{a}^\dagger\cdot\mathbf{a} + \frac{3}{2} = E/\hbar\omega$ allows us to express our spin–orbit coupled Hamiltonian as

$$H = \frac{1}{2}\{\mathcal{A}^+, \mathcal{A}^-\} + v\frac{\mathrm{i}}{\sqrt{2}}(\mathcal{A}^+ - \mathcal{A}^-). \tag{5}$$

In appendix A, we show that the matrix elements of the operators $\mathcal{A}^+$ and $\mathcal{A}^-$ are given by

$$\begin{aligned} \mathcal{A}^-|n, j, m, -\rangle &= \sqrt{2(n + j + 1)}|n, j, m, +\rangle \\ \mathcal{A}^-|n, j, m, +\rangle &= \sqrt{2n}|n - 1, j, m, -\rangle \end{aligned} \tag{6}$$

and

$$\begin{aligned} \mathcal{A}^+|n, j, m, +\rangle &= \sqrt{2(n + j + 1)}|n, j, m, -\rangle \\ \mathcal{A}^+|n, j, m, -\rangle &= \sqrt{2(n + 1)}|n + 1, j, m, +\rangle. \end{aligned} \tag{7}$$

Since the operator $\mathcal{A}^+$ contains a combination of creation operators, it is clear that it will raise the energy of a state by one unit. In the radial basis there are two ways to raise the energy by one unit. The angular quantum number can be increased by one with the radial quantum number held constant: $\Delta l = +1$, $\Delta n = 0$, or the radial number can be increases by one and the angular quantum number lowered by one. Repeated applications of the raising operator alternate between state with $l = j + s$ and $l = j - s$, while increasing the energy by one unit each time.

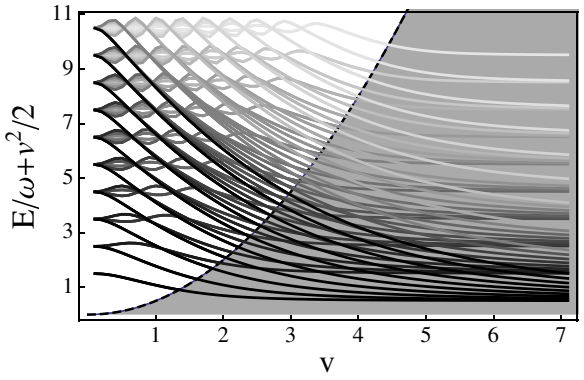

Figure 1. Numerical calculation of the spectrum as a function of v. At $v = 0$, all energy levels plotted have energy $E \leqslant 7 + \frac{3}{2}$. As the spin–orbit strength is increased, the levels split off into groups with increasing radial quantum number n. States of equal j are labelled with the same colour, with $j = \frac{1}{2}$ given by black, and $j = \frac{21}{2}$ given by the lightest grey. Each Landau level has energy of approximately $E_{njm} = (n + \frac{1}{2}) + \frac{(j+\frac{1}{2})^2}{2v^2} - \frac{v^2}{2}$. As a visual guide, each level is shifted by $v^2/2$. Two regimes are clearly identifiable, corresponding to a 3D harmonic oscillator with slight level mixing, and the quasi-1D Landau-level problem. As discussed in the text, the crossover between these two regimes is given by $E \sim v^2/2$. This crossover is shown by the black line, and the quasi-1D regime is shaded grey.

2.2. Numerical diagonalization

The spin–orbit coupled Hamiltonian can therefore be numerically diagonalized efficiently by first projecting the Hamiltonian into sectors of good $|j, m\rangle$

$$H = \sum_j \sum_{m=-j}^{j} H_{jm} |jm\rangle\langle jm| \tag{8}$$

where the Hamiltonian H_{jm} is defined by the matrix elements

$$\begin{aligned}\langle n'\lambda'|H_{jm}|n\lambda\rangle &= (2n + j + 1)\delta_{n,n'}\delta_{\lambda,\lambda'} \\ &+ \mathrm{i}v(\sqrt{n+1}\delta_{n+1,n'}\delta_{\lambda'+}\delta_{\lambda-} - \sqrt{n}\delta_{n-1,n'}\delta_{\lambda+}\delta_{\lambda'-}) \\ &+ \mathrm{i}v\sqrt{n+j+1}\delta_{n,n'}(\delta_{\lambda+}\delta_{\lambda'-} - \delta_{\lambda'+}\delta_{\lambda-}).\end{aligned} \tag{9}$$

This matrix is tridiagonal, and can be efficiently diagonalized. Figure 1 shows the spectrum as a function of the spin–orbit parameter v. At $v = 0$, we have included all states that have $N \leqslant 10$, where $N = 2n+l$ is the total quanta of the 3D isotropic oscillator. Two regions in the spectrum are identifiable. For $N \gg \frac{v^2}{2}$ the spectrum is approximately that of the 3D harmonic oscillator with $E \approx 2n + l + \frac{3}{2} - \frac{v^2}{2}$. For $N \ll \frac{v^2}{2}$ the spectrum is given by

$$E \approx \left(n + \frac{1}{2}\right) + \frac{(j+\frac{1}{2})^2}{2v^2} - \frac{v^2}{2} \tag{10}$$

as will be shown in section 2.3.3. To lowest order in $1/v$, this has the form of a one-dimensional harmonic oscillator in the radial mode. We will later see that these states are well localized in the momentum space potential near $|\mathbf{p}| = v$. This suggests that the energetically weak excitations along the polar and azimuthal directions only weakly perturbs the quasi-one-dimensional spectrum. The system therefore undergoes a dimensional reduction from $D = 3$ to $D = 1$. The one-dimensional structure is reminiscent of the Landau levels in a harmonic trap, where a radial quantum number gives well defined bands, with a weak dependence within each band upon the angular momentum quantum number. Mixing of the Landau levels appears only at higher order in the inverse spin–orbit coupling parameter. Note that while these levels have been seen in previous work, [12, 14–16], the crossover to the 3D spectrum was missed.

2.3. The Schrödinger equation as a system of coupled differential equations

2.3.1. Momentum space. The eigenstates of the Hamiltonians H_{jm} are states of good total angular momentum. In general they can be expressed as

$$|n_r, j, m\rangle = \left|\psi^+_{n_r}\right\rangle |j, m, +\rangle + \left|\psi^-_{n_r}\right\rangle |j, m, -\rangle\,, \tag{11}$$

where $\left|\psi^\pm_{n_r}\right\rangle$ is an eigenstate of H_{jm} with n_r radial modes. This form suggests that each Hamiltonian H_{jm} has a corresponding set differential equation in only the radial degrees of freedom. It is more natural to work in momentum space, where $\mathbf{p}$ is a dynamical variable, instead of an operator. The presence of the harmonic trap allows us to treat the position operator as a derivative, $\mathbf{r} = \mathrm{i}\nabla_{\mathbf{p}}$. The corresponding 'dual' Schrödinger equation is

$$\left[-\frac{\nabla^2_{\mathbf{p}}}{2} + \frac{\mathbf{p}^2}{2} + v\boldsymbol{\sigma}\cdot\mathbf{p}\right]\psi(\mathbf{p}) = E\psi(\mathbf{p}). \tag{12}$$

The radial eigenfunctions in momentum space have the corresponding form

$$\psi_{njm}(\mathbf{p}) = f^-_{nj}(p)\chi^-_{jm}(\hat{\mathbf{p}}) + f^+_{nj}(p)\chi^+_{jm}(\hat{\mathbf{p}}), \tag{13}$$

where $p = |\mathbf{p}|$, $\hat{\mathbf{p}} = \mathbf{p}/p$, $f^\pm_{nj}(p) = \langle p|\psi^\pm_{n_r}\rangle$, and the spinors $\chi^\pm_{jm} = \langle\hat{\mathbf{p}}|jm\pm\rangle$ have total momentum j, with a J_3 projection m. As shown in the appendix, the action of the operator $\boldsymbol{\sigma}\cdot\mathbf{p}$ operating on the spinors $\chi^\pm_{jm}(\hat{\mathbf{p}})$ is to interchange the spinors and multiply the result by p, i.e. $\boldsymbol{\sigma}\cdot\mathbf{p}\chi^\pm_{jm}(\hat{\mathbf{p}}) = p\chi^\mp_{jm}(\hat{\mathbf{p}})$. The form (13) gives a consistent set of two coupled differential equations in the independent variable p. These coupled differential equations takes the form

$$\begin{aligned}&\left[-\frac{1}{2}\frac{\partial^2}{\partial p^2} + \frac{1}{2}\frac{\left(j+\frac{1}{2}\right)\left(j+\frac{3}{2}\right)}{p^2} + \frac{p^2}{2}\right] \\ &\quad\times u^+_{nj}(p) + v\,p u^-_{nj}(p) = E\,u^+_{nj}(p)\end{aligned} \tag{14}$$

$$\begin{aligned}&\left[-\frac{1}{2}\frac{\partial^2}{\partial p^2} + \frac{1}{2}\frac{\left(j-\frac{1}{2}\right)\left(j+\frac{1}{2}\right)}{p^2} + \frac{p^2}{2}\right] \\ &\quad\times u^-_{nj}(p) + v\,p u^+_{nj}(p) = E\,u^-_{nj}(p)\end{aligned} \tag{15}$$

where $u^\pm_{nj}(p) = p\,f^\pm_{nj}(p)$.

The eigenfunctions $f^\pm_{nj}(p)$ can be found by solving these coupled differential equations. Alternatively, they can be constructed using the eigenvectors found from diagonalizing the projected Hamiltonians H_{jm}. Some examples of these functions are shown in figure 2 for a large v. The functions are well approximated by the one-dimensional harmonic oscillator wavefunctions centred around $p = v$.

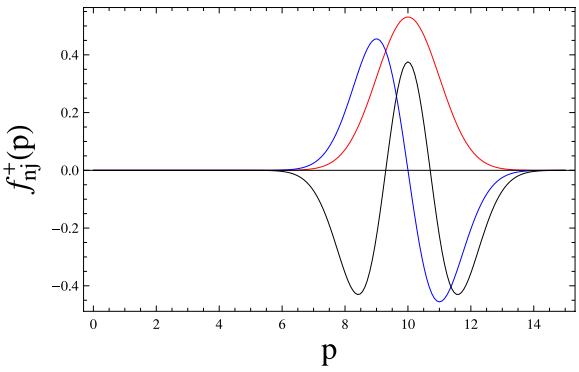

Figure 2. Momentum space eigenfunctions $f^+_{nj}(p)$ for low energy states at large spin–orbit coupling. The red, blue and black curves correspond to states with $j = \frac{1}{2}$ and $n = 1, 2, 3$ respectively. The eigenfunctions are well approximated by the one-dimensional harmonic oscillator wavefunction centred around $p = v$. The number of nodes corresponds to the radial quantum number. States with higher j have the same form, up to a possible sign, provided the number of radial quanta are smaller than $\sim v^2/2$. The eigenfunctions $f^-_{nj}(p)$ have opposite sign.

2.3.2. Position space. A radial differential equation can be found in position space in a manner analogous to the momentum space differential equations. The position space analogue of (13) is given by

$$\psi_{njm}(\mathbf{r}) = g^-_{nj}(r)\chi^-_{jm}(\hat{\mathbf{r}}) + g^+_{nj}(r)\chi^+_{jm}(\hat{\mathbf{r}}), \tag{16}$$

where $r = |\mathbf{r}|$, $\hat{\mathbf{r}} = \mathbf{r}/r$, $g^\pm_{nj}(r) = \langle r|\psi^\pm_{nj}\rangle$ and $\chi^\pm_{jm}(\hat{\mathbf{r}}) = \langle\hat{\mathbf{r}}|jm\lambda\rangle$. In the appendix we show that the functions $g^\pm_{nj}(r)$ satisfy the radial differential equation

$$\frac{1}{2}\left[-\frac{1}{r}\left(\frac{\mathrm{d}^2}{\mathrm{d}r^2}r\right) + \frac{(j+\frac{1}{2})(j+\frac{3}{2})}{r^2} + r^2\right] g^+_{nj}(r) + v\left(-\frac{\mathrm{d}}{\mathrm{d}r} + \frac{j-\frac{1}{2}}{r}\right) g^-_{nj}(r) = E_{nj} g^+_{nj}(r) \tag{17}$$

$$\frac{1}{2}\left[-\frac{1}{r}\left(\frac{\mathrm{d}^2}{\mathrm{d}r^2}r\right) + \frac{(j+\frac{1}{2})(j-\frac{1}{2})}{r^2} + r^2\right] g^-_{nj}(r) + v\left(\frac{\mathrm{d}}{\mathrm{d}r} + \frac{j+\frac{1}{2}}{r}\right) g^+_{nj}(r) = E_{nj} g^-_{nj}(r). \tag{18}$$

These differential equations can be solved to find the eigenfunctions in position space. Alternatively, we can the radial eigenfunction from the partial wave expansion found in section 2.2. Some examples of these functions are shown in figure 3 for a large v.

2.3.3. Landau levels. The Landau levels we found numerically, which are described by (10), can be understood by considering the asymptotic form of the radial differential equations, (14) and (15), in momentum space. At large momentum, $p \gtrsim v$, the $1/p^2$ term becomes negligible, and the differential equations can be decoupled by taking an even/odd superposition of (14) and (15). The two decoupled differential equations are

$$\left[-\frac{1}{2}\frac{\partial^2}{\partial p^2} + \frac{p^2}{2} \pm v\, p\right] \tilde{u}^\pm_{nj}(p) = E\, \tilde{u}^\pm_{nj}(p), \tag{19}$$

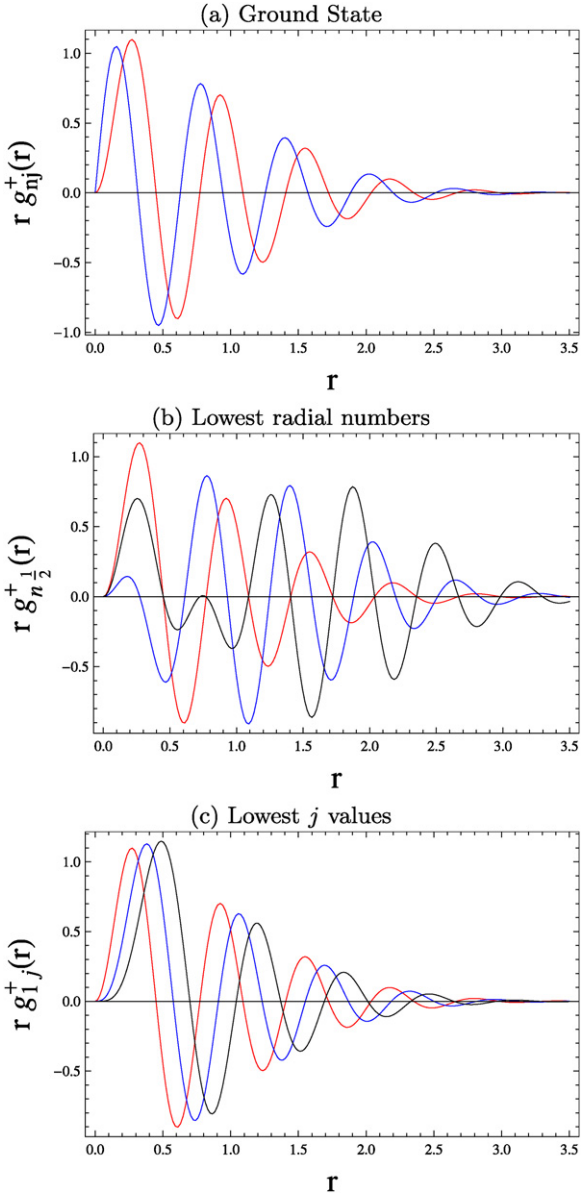

Figure 3. (a) Position space eigenfunctions for low ground states at large spin–orbit coupling. The red and blue curves correspond to the functions $rg^+_{nj}(r)$ and $rg^-_{nj}(r)$ respectively. (b) The first three position space eigenfunctions $rg^+_{nj}(r)$ for $j = 1/2$ and $n = 1, 2, 3$ (red, blue and black respectively.) (c) The position space eigenfunctions $rg^+_{nj}(r)$ in the lowest radial mode for the three lowest values of $j = \frac{1}{2}, \frac{3}{2}, \frac{5}{2}$, correspond to the red, blue and black curves respectively.

where $\tilde{u}^\pm = \frac{1}{2}(u^+ \pm u^-)$. These differential equations can be mapped to the one-dimensional harmonic oscillator by performing a change of variables $p \to p \mp v$. Away from $p = 0$, the solutions are well approximated by $\tilde{u}^\pm_{nj}(p) = c_n H_n(p \pm v)\mathrm{e}^{-\frac{(p\pm v)^2}{2}}$, where $H_n(p)$ is the nth Hermite polynomial, [31] and c_n is a normalization constant. However, the equation for $\tilde{u}^+(p)$ is localized around $p = -v$, outside of the range of definition of the radial coordinate. We therefore assume these solutions are $\tilde{u}^+_{nj}(p) = 0$. Transforming, we find that $u^+(p) = -u^-(p) = \sqrt{\frac{1}{2^n n!}}\frac{1}{\pi^{1/4}} H_n(p - v)\,\mathrm{e}^{-(p-v)^2/2}$ in the

asymptotic limit. Notice, however, that this approximation breaks down near $p \to 0$, where $u^{\pm}(p)$ must satisfy the boundary condition that $\frac{\mathrm{d}u^{\pm}}{\mathrm{d}p}\big|_{p=0} = 0$, and we therefore know that $u^{\pm}(p) \sim p^n$ as $p \to 0$.

The form of the harmonic oscillator Hamiltonian suggests the spectrum is

$$E_n = n + \frac{1}{2} - \frac{v^2}{2}. \tag{20}$$

To lowest order in v, this result is consistent with the large Landau level-like degeneracy found earlier. This degeneracy is lifted by the centrifugal barrier, which mixes the Landau levels near $p = 0$. To lowest order in perturbation theory, the energy shift in the state ψ_{njm} is given by

$$\delta E_{njm} = \langle \psi_{njm} | \frac{1}{2} \frac{\hat{l}^2}{p^2} | \psi_{njm} \rangle, \tag{21}$$

where $\hat{l}^2$ is the orbital angular momentum operator. Using (13) and the asymptotic expression for the radial wavefunction, this energy shift is

$$\delta E_{njm} = \frac{1}{4}\left[\left(j+\frac{3}{2}\right)\left(j+\frac{1}{2}\right) + \left(j+\frac{1}{2}\right)\left(j-\frac{1}{2}\right)\right] \times \frac{1}{2^n n! \sqrt{\pi}} \int_0^{\infty} \mathrm{d}p \, \frac{(H_n(p-v))^2 \, \mathrm{e}^{-(p-v)^2}}{p^2}. \tag{22}$$

Formally, the integral in (22) is divergent as $p \to 0$. This is an artefact of asymptotic approximation that does not respect the boundary condition $u' = 0$ at $p = 0$. We can cure this by introducing a low energy cutoff, and subtracting the divergent contribution. The integral is then dominated near $p = v$, and can be well approximated by $\int_0^{\infty} \mathrm{d}p \, \frac{(H_n(p-v))^2 \mathrm{e}^{-(p-v)^2}}{p^2} = \frac{2^n n! \sqrt{\pi}}{v^2} + \mathcal{O}\left(\frac{1}{v^3}\right)$, which is valid as long as $(H_n(p-v))^2 \, \mathrm{e}^{-(p-v)^2}$ is localized in a region away from $p = 0$. The lowest order shift in energies is $\delta E_{njm} = \frac{\left(j+\frac{1}{2}\right)^2}{2v^2}$, and the spectrum in the asymptotic limit is

$$E_{njm} = \left(n + \frac{1}{2}\right) + \frac{\left(j+\frac{1}{2}\right)^2}{2v^2} - \frac{v^2}{2}, \tag{23}$$

consistent with the spectrum found using numerical diagonalization in the previous section.

2.3.4. Validity of approximation. To derive (23), we considered our particle in a combination of two 'spin'-dependent potentials. The first is the centrifugal barrier, and the second is the spin–orbit coupling. The centrifugal barrier is repulsive, and divergent at $p = 0$. The spin–orbit term will form a well centred at $p = v$. For sufficiently large barriers, the minimum of the well will be far from the region where the centrifugal barrier is finite. This implies that low energy states will be well localized in the potential minimum produced by the spin–orbit coupling. Since the well is approximately harmonic near the minimum, the radial wavefunctions will be given by the one-dimensional harmonic oscillator. These states are exponentially localized near $p = v$, and will have minimum overlap with the centrifugal potential.

Wavefunctions with larger radial quantum numbers, n, will be increasingly delocalized. Since the centrifugal term acts to mix $\tilde{u}^+$ and $\tilde{u}^-$, the mixing of these states will be significant when the product of the wavefunctions $\tilde{u}^+(p)\,\tilde{u}^-(p)$ is non-negligible near $p = 0$. The product $\tilde{u}^+(p)\,\tilde{u}^-(p)$ is centred around $p = v$, and has a width that goes as $\delta p = \langle p^2 \rangle - \langle p \rangle^2 \sim \sqrt{2\left(n+\frac{1}{2}\right)}$[1]. Thus, we expect the radial Landau regime to break down when $v - \delta p \sim 0$, or accordingly $n + \frac{1}{2} \sim \frac{v^2}{2}$. For larger values of j, the spread of the wavefunction will have a small dependence on the angular quantum number, and the condition for the validity of Landau approximation becomes $E_{njm} \gtrsim 0$.

The dimensional reduction can therefore be viewed as follows: low energy states are trapped in a radial momentum-space potential well centred around $p = v$, where the spin–orbit energy $-pv$ is larger than the quadratic $p^2/2$ kinetic energy. These negative energy states are well localized in the radial direction, and only weakly mixed among the angular directions. Thus, to lowest order, only radial fluctuations may contribute to their energy. Near the crossover when $E = 0$, the momentum-space wavefunction is sufficiently delocalized such that the centrifugal term strongly mixes states with $j = l \pm s$. In this region, the kinetic term dominates the spin–orbit energy, so the spin–orbit term weakly perturbs the 3D harmonic oscillator spectrum.

3. Ground state

In the previous section we showed the momentum space ground state of a trapped particle with Weyl coupling has the approximate form

$$\psi_{0,\frac{1}{2},\pm\frac{1}{2}}(\mathbf{p}) = \frac{1}{\sqrt{2}}\left(\chi^{-}_{\frac{1}{2},\pm\frac{1}{2}}(\hat{\mathbf{p}}) - \chi^{+}_{\frac{1}{2},\pm\frac{1}{2}}(\hat{\mathbf{p}})\right)\frac{\mathrm{e}^{-(p-v)^2/2}}{\pi^{1/4}} \tag{24}$$

for $v \gg 1$. The position space wavefunction can be found using the radial differential equations. Alternatively, we can directly apply the Fourier transform to the momentum-space wavefunction, $\tilde{\psi}_0(\mathbf{r}) = \int \mathrm{d}^3\mathbf{p}\, \mathrm{e}^{\mathrm{i}\mathbf{p}\cdot\mathbf{r}} \psi_0(\mathbf{p})$. This is most easily evaluated by expanding the exponent $\mathrm{e}^{\mathrm{i}\mathbf{p}\cdot\mathbf{r}} = 4\pi \sum_{lm} i^l j_l(pr) Y_l^m(\hat{\mathbf{r}}) \left(Y_l^m(\hat{\mathbf{p}})\right)^*$. Integration over the angular coordinate converts the spinor $\chi^{\pm}_{jm}(\hat{\mathbf{p}})$ to $\chi^{\pm}_{jm}(\hat{\mathbf{r}})$. The radial component is then found from the integral $\int_0^{\infty} p^2 j_{\frac{1}{2}\pm\frac{1}{2}}(pr) \frac{\mathrm{e}^{-(p-v)^2/2}}{\pi^{1/4}} dp$. The exponential factor localizes the integrand to a region near $p \sim v$, in the asmyptotic regime with $v \gg 1$, this integral can be evaluated by extending the lower limit to $-\infty$, and then using the explicit form of the spherical Bessel functions, $j_0(x) = \frac{\sin x}{x}$ and $j_1(x) = \frac{\cos x}{x} - \frac{\sin x}{x^2}$ [32]. The position-space radial wavefunctions for the ground state are therefore given by

$$f_0(r) = \frac{\sqrt{2}}{\pi^{3/4}} \frac{1}{r} (r\cos(rv) + v\sin(rv))\, \mathrm{e}^{-r^2/2} \tag{25}$$

$$f_1(r) = \frac{\sqrt{2}}{\pi^{3/4}} \frac{1}{r^2} ((1+r^2)\sin(rv) - rv\cos(rv))\, \mathrm{e}^{-r^2/2} \tag{26}$$

[1] This is in contrast to the wavefunction $\tilde{u}^-(p)$ that has width $\delta p \sim \sqrt{n+\frac{1}{2}}$. Notice also that the product $\tilde{u}^+\tilde{u}^-$ is suppressed in amplitude as e^{-v^2} for small n, but will have a significant contribution near $p = 0$ for larger n.

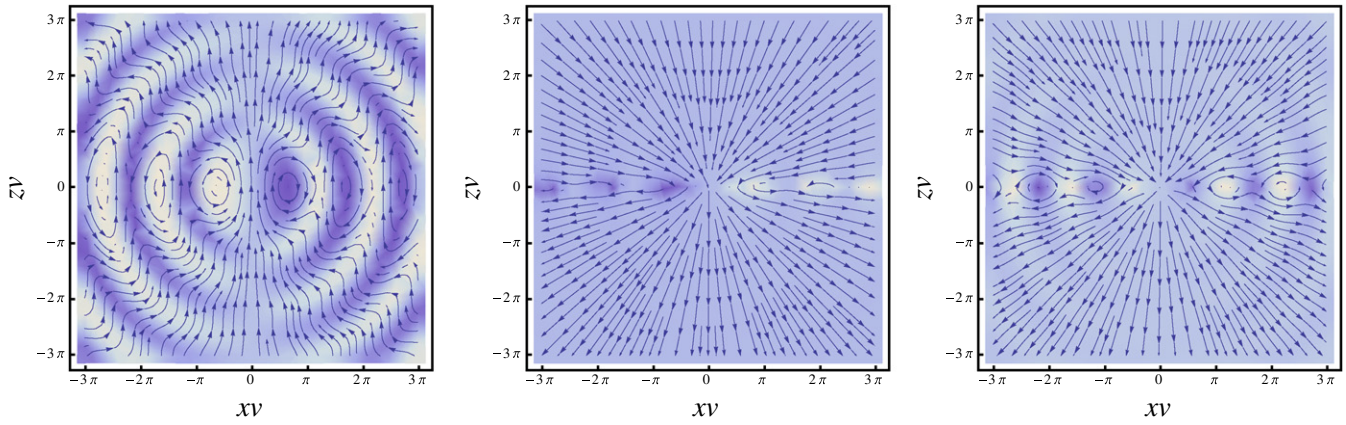

(a) Spin current (b) Orbital current (c) Total current

Figure 4. The currents $\mathbf{j}_s$, $\mathbf{j}_o$ and $\mathbf{j} = \mathbf{j}_s + \mathbf{j}_o$, for the ground state of a trapped particle with Weyl coupling, with $j = \frac{1}{2}$, $m = \frac{1}{2}$ and $v = 10$. For clarity, we have scaled the currents $\mathbf{j}_i$ by e^{r^2} to account for the Gaussian damping of the wavefunction, and measured distance in units of $1/v$, the spin–orbit length. In all figures the plane defined by $y = 0$ is plotted. The arrows represent flows of the local normalized current vector. The colour density represents the out-of-plane component of the spin textures, with lightest colour representing the maximal out-of-plane current, and the darkest representing maximal in-plane current. All three currents are azimuthally symmetric. (a) The spin currents, $\mathbf{j}_s$, have oscillations on the length scale $r \sim 2\pi/v$. On the axis with $z = 0$, the local spin vector is polarized entirely out-of-plane at solutions to $\tan rv = -rv/v^2$. For large v, the solutions are given approximately by $rv = n\pi$, where n is an integer. The odd solutions feature in-plane vortex loops of spin, while the spin forms anti-vortices at the even solutions. (b) The orbital currents, $\mathbf{j}_o$, are dominated by the in-plane component, which is stronger than the out-of-plane components by a factor of v. A small out-of-plane component is largest on the $z = 0$ axis. In the upper half plane with $y > 0$, current converges on the point $r = 0$, while on the lower half plane all the current diverges away from the point $r = 0$. (c) The total current, $\mathbf{j}$, is the sum of orbital and spin currents. The contributions from spin and orbital degrees of freedom are conserved independently.

with asymptotic corrections of $\mathcal{O}(1/v^2)$. The full position space wavefunction is approximately given by

$$\psi_{0,\frac{1}{2},\pm\frac{1}{2}}(\mathbf{r}) = \tfrac{1}{\sqrt{2}}\big(f_0(r)\chi^-_{\frac{1}{2},\pm\frac{1}{2}}(\hat{\mathbf{r}}) - if_1(r)\chi^+_{\frac{1}{2},\pm\frac{1}{2}}(\hat{\mathbf{r}})\big) \quad (27)$$

in the asymptotic limit.

3.1. Spin textures and currents

3.1.1. Momentum space. The azimuthal component of the spinor $\chi^+_{\frac{1}{2}\frac{1}{2}}$ suggests the Weyl coupling should have a non-zero current in the ground state. We first define the current operator in momentum space in the standard way. First we multiply Schrödinger's equation by $\psi^\dagger$, $-\mathrm{i}\psi^\dagger\frac{\partial}{\partial t}\psi = \psi^\dagger\big[-\frac{\nabla_{\mathbf{p}}^2}{2}+\frac{\mathbf{p}^2}{2}\big]\psi + v\mathbf{p}\cdot(\psi^\dagger\boldsymbol{\sigma}\psi)$, and subtract the result from it's complex conjugate. The momentum-space continuity equation is

$$\partial_t\left(\psi^\dagger\psi\right) = -\nabla_{\mathbf{p}}\cdot\mathbf{j}_{\mathbf{p}} \quad (28)$$

where

$$\mathbf{j}_{\mathbf{p}} = \left(-\frac{\mathrm{i}}{2}\right)[\psi^\dagger\nabla_{\mathbf{p}}\psi - \psi^T\nabla_{\mathbf{p}}\psi^*] = \Im[\psi^\dagger\nabla_{\mathbf{p}}\psi] \quad (29)$$

is the momentum-space current density. We find that the ground state current in momentum space is given by

$$\mathbf{j}_{\mathbf{p}} = \pm\frac{\sin\theta}{p}\frac{\mathrm{e}^{-(p-v)^2}}{4\pi}\hat{\phi} \quad (30)$$

for a state with $m = \pm\frac{1}{2}$.

3.1.2. Position space. In position space, the spin–orbit coupling is imaginary, so the continuity equation will have contributions from the orbital and spin degrees of freedom:

$$\mathbf{j} = \mathbf{j}_0 + \mathbf{j}_s \quad (31)$$

where the orbital contribution $\mathbf{j}_0 = \Im[\psi^\dagger\nabla\psi]$ is the standard current operator, and the component due to spin is $\mathbf{j}_s = v(\psi^\dagger\boldsymbol{\sigma}\psi)$. We call $\mathbf{j}_0$ and $\mathbf{j}_s$ the 'orbital' and 'spin' currents respectively[2]. For an eigenstate of the trapped Weyl Hamiltonian, both contributions are azimuthally symmetric: that is the current fields do not change forms under a rotation by ϕ. Both currents can be calculated exactly for the ground state in the large spin–orbit limit, and are given by

$$\mathbf{j}_0 = \frac{1}{4\pi}\Big[\left(f_0^+\partial_r f_0^- - f_0^-\partial_r f_0^+\right)\cos\theta\hat{r} + \sin\theta\frac{f_0^+}{r}\left(f_0^-\hat{\theta} + f_0^+\hat{\phi}\right)\Big] \quad (32)$$

$$\mathbf{j}_s = \frac{v}{4\pi}\big[\left(\left(f_0^+\right)^2\cos\theta - \left(f_0^-\right)^2\sin\theta\right)\hat{r} + \left(\left(f_0^+\right)^2\sin\theta + \left(f_0^-\right)^2\cos\theta\right)\hat{\theta} + \left(2f_0^+f_0^-\sin\theta\right)\hat{\phi}\big] \quad (33)$$

for the ground state $j = \frac{1}{2}$ and $m = \frac{1}{2}$. These currents are shown in figure 4. Since the length scale $1/v$ appears only in the radial variable, the radial component of the orbital current will be stronger than the polar and azimuthal component by a factor

[2] This definition of spin current differs from the standard definition that satisfies the vector continuity equation $\partial_t S_i = -\nabla\cdot\mathbf{j}_i$, where $\mathbf{S} = \frac{1}{2}\psi^\dagger\boldsymbol{\sigma}\psi$ is the expectation value of the spin operator, and $\mathbf{j}$ is now a tensor. In fact, since the spin operator does not commute with the Hamiltonian, spin is not a conserved quantity and it does not make sense to define such an operator.

of v. As is seen in figure 4(b), the out-of-plane component of spin is negligible only near the plane defined by $\theta = \pi/2$. The lower half-plane has all currents flowing to the point $r = 0$, while all currents in the upper half plane diverge from this point. The sum of the two currents is seen in figure 4(c). Explicit calculation shows that the contribution to the total current from both the spin and orbital terms are independently conserved, and thus the total current is also conserved.

The spin currents do have an out-of-plane, or azimuthal, component of spin. The in-plane component has a similar structure to the orbital current, in the lower half-plane the current converges to $r = 0$, while it diverges from the point $r = 0$ in the upper half plane. At small spin–orbit coupling, $v \ll 1$, the Gaussian factor damps the wavefunction before significant spin oscillations can occur, and the spin current is everywhere polarized along the $\hat{z}$-axis. When $v \sim 1$, the spin current in the $z = 0$ plane will become entirely azimuthally polarized at one value of r. In the large $v \gg 1$ limit, the out-of-plane component oscillates on the scale $r \sim 2\pi/v$ with amplitude $\cos\theta$. At special points corresponding to the solutions of $\tan rv = -rv/v^2$, the out-of-plane spin current is completely polarized in the azimuthal direction.

4. Conclusion

The problem of the three-dimensional spin–orbit coupling in a harmonic trap was considered. The system has a conserved total angular momentum that allows the Hamiltonian to be projected into sectors where j, m are good quantum numbers. Each sector is tri-diagonal, providing for an efficient numerical calculation of the spectrum. At large values of the spin–orbit coupling parameter, the system undergoes a dimensional reduction from three to one. The spectrum is well approximated by Landau levels in the radial coordinate, with splittings inversely proportional the spin–orbit coupling strength.

The conservation of total angular momentum allows us to express Schrödinger's equation as a set of coupled differential equations in the radial coordinate. We find the form of these differential equations in both position and momentum space. Using asymptotic analysis on the momentum space differential equations, we reproduce an analytic spectrum that well approximates the spectrum found numerically. We further use this approximation to find analytical expressions for the low energy eigenfunctions in both position and momentum space.

Finally, we explore the properties of the ground state wavefunction. We find a momentum space orbital current in the azimuthal direction. In position space the total current can be decomposed into a spin current and an orbital current. All currents are invariant under azimuthal rotation. At large spin–orbit coupling, the spin currents have an azimuthal component that oscillates on the inverse of the spin–orbit strength. Along the $z = 0$ axis, the spin currents alternate between complete polarization with and against the azimuthal plane. At these special points, the in plane spin density has vortex and anti-vortex structure. The orbital current is characterized by a convergence of all currents at the point $r = 0$ in the upper half-sphere, with a divergence of away from the same point in the lower half-sphere.

Acknowledgments

During the completion of this manuscript, the authors became aware of two similar works a system with Weyl spin–orbit coupling [33, 34]. This research was performed in part under the sponsorship of the US Department of Commerce, National Institute of Standards and Technology, and was supported by the National Science Foundation under Physics Frontiers Center Grant PHY-0822671 and by the ARO under the DARPA OLE program.

Appendix A.

In this appendix we show that $\mathcal{A}^+$ and $\mathcal{A}^-$ have the matrix elements as described by equation (6) and (7). To do this, we first need to calculate the matrix elements of the three-dimensional isotropic harmonic oscillator basis, $\langle n'l'm'|a_q|nlm\rangle$ and $\langle n'l'm'|a_q^\dagger|nlm\rangle$, where $q = 0, \pm 1$, and the states $|nlm\rangle$ are the states three-dimensional harmonic oscillator basis as defined in the main text.

It is convenient to define the number basis $|n, l, m_l\rangle$ where (n, l, m_l) are respectively the radial, angular and magnetic quantum numbers. In the absence of spin–orbit coupling we have the harmonic oscillator energies $E = \hbar\omega\left(2n + l + \frac{3}{2}\right)$ where a state of angular momentum l has a $2l + 1$-fold degeneracy of m_l. To do this we define the spherical creation and annihilation operators $a_\pm = \mp\frac{1}{\sqrt{2}}(a_x \mp \mathrm{i}a_y)$, $a_\pm^\dagger = \mp\frac{1}{\sqrt{2}}\left(a_x^\dagger \pm \mathrm{i}a_y^\dagger\right)$, and $a_0 = a_z$, $a_0^\dagger = a_z^\dagger$. We will find it helpful to express the angular momentum generators as

$$L_+ = \sqrt{2}\left(a_+^\dagger a_z + a_z^\dagger a_-\right), \tag{A.1}$$

$$L_- = \sqrt{2}\left(a_-^\dagger a_z + a_z^\dagger a_+\right), \tag{A.2}$$

$$L_z = a_+^\dagger a_+ - a_-^\dagger a_- \tag{A.3}$$

with $L_x = \frac{1}{2}(L_+ + L_-)$ and $L_y = -\frac{\mathrm{i}}{2}(L_+ - L_-)$. If we additionally define the operators

$$S_+ = \frac{1}{2}\left(a_0^\dagger\right)^2 - a_+^\dagger a_-^\dagger \tag{A.4}$$

$$S_- = \frac{1}{2}(a_0)^2 - a_+ a_- \tag{A.5}$$

$$S_0 = \frac{1}{2}\left(\hat{N} + \frac{3}{2}\right). \tag{A.6}$$

These operators commute with the angular momentum operators, and satisfy the commutation relations $[S_+, S_-] = -2S_0$ and $[S_0, S_\pm] = \pm S_\pm$. The three-dimensional harmonic oscillator eigenstates can be expressed as

$$|nlm\rangle = \left[\frac{\Gamma\left(l + \frac{3}{2}\right)}{n!\Gamma\left(n + l + \frac{3}{2}\right)}\frac{(l+m)!}{(2l)!(l-m)!}\right] S_+^n L_-^{l-m}|0, l, l\rangle \tag{A.7}$$

where $|0, l, l\rangle = \frac{1}{\sqrt{l!}}\left(a_+^\dagger\right)^l|0, 0, 0\rangle$ is a state of maximum angular momentum. It can be seen that a state $|nlm\rangle$ has energy $E = 2n + l + \frac{3}{2}$.

A.1. Calculation of: $a_q^\dagger$

To calculate $a_-^\dagger$, we first note that the operator changes the total energy number by $\Delta n = +1$ unit, so it must connect states with either $\Delta n = +1$ and $\Delta l = -1$, or $\Delta n = 0$ and $\Delta l = +1$. Other states with $\Delta n > 1$ and $\Delta l = -1+2(\Delta n-1)$ are consistent with this condition, but must have zero matrix elements from the fact that a_q is a spherical tensor of rank-1, and higher order corrections are inconsistent with angular momentum conservation. Using this fact, the matrix elements can be decomposed as

$$\langle n', l', m'|a_-^\dagger|n, l, m\rangle = \langle n, l+1, m-1|a_-^\dagger|n, l, m\rangle\delta_{n',n}\delta_{l',l+1}\delta_{m',m-1} \quad (A.8)$$

$$+ \langle n+1, l-1, m-1|a_-^\dagger|n, l, m\rangle\delta_{n',n+1}\delta_{l',l-1}\delta_{m',m-1} \quad (A.9)$$

The two non-zero elements can be calculated individually. We first calculate $\langle n, l+1, m-1|a_-^\dagger|n, l, m\rangle$. It is convenient to use the equivalent definition of $|n, l, m\rangle$, given by

$$|nlm\rangle = \left[\frac{\Gamma\left(l+\frac{3}{2}\right)}{n!\Gamma\left(n+l+\frac{3}{2}\right)}\frac{(l-m)!}{(2l)!(l+m)!}\right]S_+^n L_-^{l+m}|0, l, -l\rangle \quad (A.10)$$

to express the desired element as

$$\langle n, l+1, m-1|a_-^\dagger|n, l, m\rangle = \tilde{\mathcal{N}}_{n,l+1,m-1}\tilde{\mathcal{N}}_{n,l,m}\langle\mathbf{0}|(a_-)^{l+1} \times (L_-)^{l+m}(S_-)^n a_-^\dagger (S_+)^n (L_+)^{l+m}(a_-^\dagger)^l|\mathbf{0}\rangle \quad (A.11)$$

$$= \tilde{\mathcal{N}}_{n,l+1,m-1}\tilde{\mathcal{N}}_{n,l,m}\langle\mathbf{0}|(a_-)^{l+1}(L_-)^{l+m}(S_-)^n \times (S_+)^n a_-^\dagger (L_+)^{l+m}(a_-^\dagger)^l|\mathbf{0}\rangle \quad (A.12)$$

where the normalization constant is $\tilde{\mathcal{N}}_{n,l,m} = \left[\frac{\Gamma(l+\frac{3}{2})}{n!\Gamma(n+l+\frac{3}{2})}\frac{(l-m)!}{(2l)!(l+m)!}\right]$, and we have used the commutation relation $[a_-^\dagger, S_+] = 0$. The bra $\langle 0|(a_-)^{l+1}(L_-)^{l+m}$ is an eigenbra of the operator $(S_-)^n(S_+)^n$ with eigenvalue $\frac{n!\Gamma(n+l+3/2+1)}{\Gamma(l+3/2+1)}$. We can again use the commutation of the operator $[L_-, a_-^\dagger] = 0$ to find the remaining factor

$$\langle\mathbf{0}|(a_-)^{l+1}(L_-)^{l+m}a_-^\dagger(L_+)^{l+m}(a_-^\dagger)^l|\mathbf{0}\rangle = \langle\mathbf{0}|(a_-)^{l+1}a_-^\dagger(L_-)^{l+m}(L_+)^{l+m}(a_-^\dagger)^l|\mathbf{0}\rangle \quad (A.13)$$

$$= (l+1)\langle\mathbf{0}|(a_-)^l(L_-)^{l+m}(L_+)^{l+m}(a_-^\dagger)^l|\mathbf{0}\rangle \quad (A.14)$$

$$= (l+1)\tilde{\mathcal{N}}_{0,l,m}^{-2}. \quad (A.15)$$

These factors combine to give the non-zero value of the matrix element

$$\langle n, l+1, m-1|a_-^\dagger|n, l, m\rangle = \frac{1}{2}\sqrt{\frac{n+l+3/2}{l+3/2}\frac{(l-m+2)(l-m+1)}{l+1/2}}. \quad (A.16)$$

Similar techniques can applied to evaluate the other non-zero matrix element of the operator $a_-^\dagger$. The calculation is straightforward using the same techniques. The full matrix element is given by

$$\langle n', l', m'|a_-^\dagger|n, l, m\rangle = \frac{1}{2}\sqrt{\frac{n+l+3/2}{l+3/2}\frac{(l-m+2)(l-m+1)}{l+1/2}} \times \delta_{n',n}\delta_{l',l+1}\delta_{m',m-1} \quad (A.17)$$

$$- \frac{1}{2}\sqrt{\frac{n+1}{l+1/2}\frac{(l+m)(l+m-1)}{l-1/2}}\delta_{n',n+1}\delta_{l',l-1}\delta_{m',m-1}. \quad (A.18)$$

The remaining matrix elements can be calculated in an analogous way. The results can be summarized by the expression

$$a_q^\dagger|n, l, m\rangle = c_q^+(n, l, m)|n, l+1, m+q\rangle + d_q^+(n, l, m)|n+1, l-1, m+q\rangle \quad (A.19)$$

where $q = -1, 0, 1$, and the matrix elements are given by

$$c_q^-(n, l, m) = \left(\frac{1}{\sqrt{2}}\right)^{1+|q|}\sqrt{\frac{n+l+1/2}{(l+1/2)(l-1/2)}}f_q(l, m) \quad (A.20)$$

$$d_q^-(n, l, m) = (-1)^q\left(\frac{1}{\sqrt{2}}\right)^{1+|q|} \times \sqrt{\frac{n}{(l+3/2)(l+1/2)}}g_{-q}(l, m) \quad (A.21)$$

$$c_q^+(n, l, m) = \left(\frac{1}{\sqrt{2}}\right)^{1+|q|}\sqrt{\frac{n+l+3/2}{(l+3/2)(l+1/2)}}g_q(l, m) \quad (A.22)$$

$$d_q^+(n, l, m) = (-1)^q\left(\frac{1}{\sqrt{2}}\right)^{1+|q|} \times \sqrt{\frac{n+1}{(l+1/2)(l-1/2)}}f_{-q}(l, m) \quad (A.23)$$

where the functions $f_q(l, m)$ and $g_q(l, m)$ are defined as

$$f_q(l, m) = \begin{cases}\sqrt{(l+m)(l+m-1)} & q = +1\\ \sqrt{(l+m)(l-m)} & q = 0\\ \sqrt{(l-m)(l-m-1)} & q = -1\end{cases} \quad (A.24)$$

$$g_q(l, m) = \begin{cases}\sqrt{(l+m+2)(l+m+1)} & q = +1\\ \sqrt{(l+m+1)(l-m+1)} & q = 0\\ \sqrt{(l-m+2)(l-m+1)} & q = -1.\end{cases} \quad (A.25)$$

The matrix elements of the operators a_q can be calculated through conjugation.

A.2. Matrix elements of $\mathcal{A}^+$ *and* $\mathcal{A}^-$.

We can now calculate the matrix elements of $\mathcal{A}^+$ and $\mathcal{A}^-$ for states of good total angular momentum labelled by quantum numbers j, m. Recall in the main text that these states are defined by

$$|n, j, m, \lambda\rangle = e^{i\phi_\lambda}\begin{pmatrix}\lambda\sqrt{\frac{j-\lambda m+x_\lambda}{2(j+x_\lambda)}}\left|n, j+\frac{\lambda}{2}, m-\frac{1}{2}\right\rangle\\ -\sqrt{\frac{j+\lambda m+x_\lambda}{2(j+x_\lambda)}}\left|n, j+\frac{\lambda}{2}, m+\frac{1}{2}\right\rangle\end{pmatrix} \quad (A.26)$$

where ϕ_λ is an arbitrary phase and $x_\lambda = \frac{1+\lambda}{2}$. We will find it convenient to express this as

$$|n,\, j,\, m,\, \lambda\rangle = \begin{pmatrix} \gamma_\lambda^{\uparrow} \left| n,\, j+\frac{\lambda}{2},\, m-\frac{1}{2} \right\rangle \\ \gamma_\lambda^{\downarrow} \left| n,\, j+\frac{\lambda}{2},\, m+\frac{1}{2} \right\rangle \end{pmatrix}, \tag{A.27}$$

where $\gamma_\lambda^{\uparrow} = \lambda e^{i\phi_\lambda}\sqrt{\frac{j-\lambda m+x_\lambda}{2(j+x_\lambda)}}$ and $\gamma_\lambda^{\downarrow} = -e^{i\phi_\lambda}\sqrt{\frac{j+\lambda m+x_\lambda}{2(j+x_\lambda)}}$.

We now consider the action of the operator $\boldsymbol{\sigma}\cdot\mathbf{p}$ on the states $|n,\, j,\, m,\, \lambda\rangle$,

$$\mathbf{p}\cdot\boldsymbol{\sigma}|n,\, j,\, m,\, \lambda\rangle = (\sqrt{2}(\sigma_- a_- - \sigma_+ a_+) + \sigma_z a_z)|n,\, j,\, m,\, \lambda\rangle \tag{A.28}$$

$$= \begin{pmatrix} -\sqrt{2}\gamma_\lambda^{\downarrow} a_+ \left| n,\, j+\frac{\lambda}{2},\, m+\frac{1}{2} \right\rangle + \gamma_\lambda^{\uparrow} a_z \left| n,\, j+\frac{\lambda}{2},\, m-\frac{1}{2} \right\rangle \\ \sqrt{2}\gamma_\lambda^{\uparrow} a_- \left| n,\, j+\frac{\lambda}{2},\, m-\frac{1}{2} \right\rangle - \gamma_\lambda^{\downarrow} a_z \left| n,\, j+\frac{\lambda}{2},\, m+\frac{1}{2} \right\rangle \end{pmatrix} \tag{A.29}$$

$$= \begin{pmatrix} \left(-\sqrt{2}\gamma_\lambda^{\downarrow} c_+^- \left(n,\, j+\frac{\lambda}{2},\, m+\frac{1}{2} \right) + \gamma_\lambda^{\uparrow} c_0^- \left(n,\, j+\frac{\lambda}{2},\, m-\frac{1}{2} \right) \right) \left| n,\, j-1+\frac{\lambda}{2},\, m-\frac{1}{2} \right\rangle \\ \left(\sqrt{2}\gamma_\lambda^{\uparrow} c_-^- \left(n,\, j+\frac{\lambda}{2},\, m-\frac{1}{2} \right) - \gamma_\lambda^{\downarrow} c_0^- \left(n,\, j+\frac{\lambda}{2},\, m+\frac{1}{2} \right) \right) \left| n,\, j-1+\frac{\lambda}{2},\, m+\frac{1}{2} \right\rangle \end{pmatrix} \tag{A.30}$$

$$+ \begin{pmatrix} \left(-\sqrt{2}\gamma_\lambda^{\downarrow} d_+^- (n,\, j+\frac{\lambda}{2},\, m+\frac{1}{2}) + \gamma_\lambda^{\uparrow} d_0^- (n,\, j+\frac{\lambda}{2},\, m-\frac{1}{2}) \right) |n-1,\, j+1+\frac{\lambda}{2},\, m-\frac{1}{2}\rangle \\ \left(\sqrt{2}\gamma_\lambda^{\uparrow} d_-^- (n,\, j+\frac{\lambda}{2},\, m-\frac{1}{2}) - \gamma_\lambda^{\downarrow} d_0^- (n,\, j+\frac{\lambda}{2},\, m+\frac{1}{2}) \right) |n-1,\, j+1+\frac{\lambda}{2},\, m+\frac{1}{2}\rangle \end{pmatrix}. \tag{A.31}$$

This can be expressed as

$$\begin{aligned} &(\sqrt{2}(\sigma_- a_- - \sigma_+ a_+) + \sigma_z a_z)|n,\, j,\, m,\, \lambda\rangle \\ &= \begin{pmatrix} \Gamma_c^{\uparrow}(\lambda) \left| n,\, j-1+\frac{\lambda}{2},\, m-\frac{1}{2} \right\rangle \\ \Gamma_c^{\downarrow}(\lambda) \left| n,\, j-1+\frac{\lambda}{2},\, m+\frac{1}{2} \right\rangle \end{pmatrix} \\ &\quad + \begin{pmatrix} \Gamma_d^{\uparrow}(\lambda) \left| n-1,\, j+1+\frac{\lambda}{2},\, m-\frac{1}{2} \right\rangle \\ \Gamma_d^{\downarrow}(\lambda) \left| n-1,\, j+1+\frac{\lambda}{2},\, m+\frac{1}{2} \right\rangle \end{pmatrix}, \end{aligned} \tag{A.32}$$

where the coefficients

$$\begin{aligned} \Gamma_c^{\uparrow}(\lambda) &= \left(-\sqrt{2}\gamma_\lambda^{\downarrow} c_+^- \left(n,\, j+\frac{\lambda}{2},\, m+\frac{1}{2} \right) \right. \\ &\quad \left. + \gamma_\lambda^{\uparrow} c_0^- \left(n,\, j+\frac{\lambda}{2},\, m-\frac{1}{2} \right) \right) \\ &= -e^{i\phi_\lambda}\sqrt{\frac{n+j+\frac{\lambda}{2}+\frac{1}{2}}{2\left(j+\frac{\lambda}{2}+\frac{1}{2}\right)\left(j+\frac{\lambda}{2}-\frac{1}{2}\right)}} \\ &\quad \times \left(-f_+ \left(j+\frac{\lambda}{2},\, m+\frac{1}{2} \right)\gamma_\lambda^{\downarrow} \right. \\ &\quad \left. + f_0 \left(j+\frac{\lambda}{2},\, m-\frac{1}{2} \right)\gamma_\lambda^{\uparrow} \right) \\ &= e^{i\phi_\lambda}\sqrt{\frac{(n+j+x_\lambda)(j+m+x_\lambda-1)}{4(j+x_\lambda)^2(j+x_\lambda-1)}} \\ &\quad \times (\sqrt{(j+\lambda m+x_\lambda)(j+m+x_\lambda)} \\ &\quad + \lambda\sqrt{(j-\lambda m+x_\lambda)(j-m+x_\lambda)}) \end{aligned} \tag{A.33}$$

and

$$\begin{aligned} \Gamma_c^{\downarrow}(\lambda) &= \left(\sqrt{2}\gamma_\lambda^{\uparrow} c_-^- \left(n,\, j+\frac{\lambda}{2},\, m-\frac{1}{2} \right) \right. \\ &\quad \left. - \gamma_\lambda^{\downarrow} c_0^- \left(n,\, j+\frac{\lambda}{2},\, m+\frac{1}{2} \right) \right) \\ &= -e^{i\phi_\lambda}\sqrt{\frac{n+j+\frac{\lambda}{2}+\frac{1}{2}}{2\left(j+\frac{\lambda}{2}+\frac{1}{2}\right)\left(j+\frac{\lambda}{2}-\frac{1}{2}\right)}} \\ &\quad \times \left(-f_- \left(j+\frac{\lambda}{2},\, m-\frac{1}{2} \right)\gamma_\lambda^{\uparrow} \right. \\ &\quad \left. - f_0 \left(j+\frac{\lambda}{2},\, m+\frac{1}{2} \right)\gamma_\lambda^{\downarrow} \right) \\ &= e^{i\phi_\lambda}\sqrt{\frac{(n+j+x_\lambda)(j-m+x_\lambda-1)}{4(j+x_\lambda)^2(j+x_\lambda-1)}} \\ &\quad \times (\lambda\sqrt{(j-\lambda m+x_\lambda)(j-m+x_\lambda)} \\ &\quad + \sqrt{(j+\lambda m+x_\lambda)(j+m+x_\lambda)}). \end{aligned} \tag{A.34}$$

Explicitly calculating these for $\lambda = \pm 1$ we get:

$$\begin{aligned} &\left(\sqrt{2}\gamma_+^{\downarrow} c_+^- \left(n,\, j+\frac{1}{2},\, m+\frac{1}{2} \right) + \gamma_+^{\uparrow} c_0^- \left(n,\, j+\frac{1}{2},\, m-\frac{1}{2} \right) \right) \\ &\quad = e^{i\phi_+}\sqrt{2(n+j+1)}\sqrt{\frac{j+m}{2j}} \end{aligned} \tag{A.35}$$

$$\begin{aligned} &\left(\sqrt{2}\gamma_-^{\downarrow} c_+^- \left(n,\, j-\frac{1}{2},\, m+\frac{1}{2} \right) \right. \\ &\quad \left. + \gamma_-^{\uparrow} c_0^- \left(n,\, j-\frac{1}{2},\, m-\frac{1}{2} \right) \right) = 0 \end{aligned} \tag{A.36}$$

and

$$\begin{aligned} &\left(\sqrt{2}\gamma_+^{\uparrow} c_-^- \left(n,\, j+\frac{1}{2},\, m-\frac{1}{2} \right) - \gamma_+^{\downarrow} c_0^- \left(n,\, j+\frac{1}{2},\, m+\frac{1}{2} \right) \right) \\ &\quad = e^{i\phi_+}\sqrt{2(n+j+1)}\sqrt{\frac{j-m}{2j}} \end{aligned} \tag{A.37}$$

$$\begin{aligned} &\left(\sqrt{2}\gamma_-^{\uparrow} c_-^- \left(n,\, j-\frac{1}{2},\, m-\frac{1}{2} \right) \right. \\ &\quad \left. - \gamma_-^{\downarrow} c_0^- \left(n,\, j-\frac{1}{2},\, m+\frac{1}{2} \right) \right) = 0. \end{aligned} \tag{A.38}$$

Similarly, we calculate the equivalent terms for $\Gamma_d^s(\lambda)$ with $s = \uparrow, \downarrow$. This gives

$$\begin{aligned} \Gamma_d^{\uparrow}(\lambda) &= \left(-\sqrt{2}\gamma_\lambda^{\downarrow} d_+^- \left(n,\, j+\frac{\lambda}{2},\, m+\frac{1}{2} \right) \right. \\ &\quad \left. + \gamma_\lambda^{\uparrow} d_0^- \left(n,\, j+\frac{\lambda}{2},\, m-\frac{1}{2} \right) \right) \end{aligned} \tag{A.39}$$

$$\begin{aligned} &= e^{i\phi_\lambda}\sqrt{\frac{n(j-m+x_\lambda+1)}{4(j+x_\lambda)^2(j+x_\lambda+1)}} \\ &\quad \times (\sqrt{(j+\lambda m+x_\lambda)(j-m+x_\lambda)} \\ &\quad - \lambda\sqrt{(j-\lambda m+x_\lambda)(j+m+x_\lambda)}) \end{aligned} \tag{A.40}$$

$$\begin{aligned} \Gamma_d^{\downarrow}(\lambda) &= \left(\sqrt{2}\gamma_\lambda^{\uparrow} d_-^- \left(n,\, j+\frac{\lambda}{2},\, m-\frac{1}{2} \right) \right. \\ &\quad \left. - \gamma_\lambda^{\downarrow} d_+^0 \left(n,\, j+\frac{\lambda}{2},\, m+\frac{1}{2} \right) \right) \end{aligned} \tag{A.41}$$

$$= -e^{i\phi_\lambda}\sqrt{\frac{n(j+m+x_\lambda+1)}{4(j+x_\lambda)^2(j+x_\lambda+1)}} \times (\lambda\sqrt{(j-\lambda m+x_\lambda)(j+m+x_\lambda)} - \sqrt{(j-m+x_\lambda)(j+\lambda m+x_\lambda)}) \quad (A.42)$$

Explicitly,

$$\Gamma_d^\uparrow(+) = \left(-\sqrt{2}\gamma_+^\downarrow d_+^-\left(n, j+\frac{1}{2}, m+\frac{1}{2}\right) + \gamma_+^\uparrow d_0^-\left(n, j+\frac{1}{2}, m-\frac{1}{2}\right)\right) = 0 \quad (A.43)$$

$$\Gamma_d^\uparrow(-) = \left(-\sqrt{2}\gamma_-^\downarrow d_+^-\left(n, j-\frac{1}{2}, m+\frac{1}{2}\right) + \gamma_-^\uparrow d_0^-\left(n, j-\frac{1}{2}, m-\frac{1}{2}\right)\right) = e^{i\phi_-}\sqrt{2n}\sqrt{\frac{j-m+1}{2(j+1)}} \quad (A.44)$$

$$\Gamma_d^\downarrow(+) = \left(\sqrt{2}\gamma_+^\uparrow d_-^-\left(n, j+\frac{1}{2}, m-\frac{1}{2}\right) - \gamma_+^\downarrow d_+^0\left(n, j+\frac{1}{2}, m+\frac{1}{2}\right)\right) = 0 \quad (A.45)$$

$$\Gamma_d^\downarrow(-) = \left(\sqrt{2}\gamma_-^\uparrow d_-^-\left(n, j-\frac{1}{2}, m-\frac{1}{2}\right) - \gamma_-^\downarrow d_+^0\left(n, j-\frac{1}{2}, m+\frac{1}{2}\right)\right) = e^{i\phi_-}\sqrt{2n}\sqrt{\frac{j+m+1}{2(j+1)}} \quad (A.46)$$

We summarize these relations as (restoring the subscript on n_r)

$$\mathcal{A}^-|n_r, j, m, +\rangle = e^{i\Delta\phi}\sqrt{2n_r}|n_r-1, j, m, -\rangle \quad (A.47)$$

$$\mathcal{A}^-|n_r, j, m, -\rangle = e^{-i\Delta\phi}\sqrt{2(n_r+j+1)}|n_r, j, m, +\rangle \quad (A.48)$$

where $\Delta\phi = (\phi_+ - \phi_-)$. We can find the action of the operator $\mathcal{A}^+ = \mathcal{A}^{-\dagger}$ through conjugation

$$\mathcal{A}^+|n_r, j, m, +\rangle = e^{-i\Delta\phi}\sqrt{2(n_r+j+1)}|n_r, j, m, -\rangle \quad (A.49)$$

$$\mathcal{A}^+|n_r, j, m, -\rangle = e^{i\Delta\phi}\sqrt{2(n_r+1)}|n_r+1, j, m, +\rangle \quad (A.50)$$

We can show that $\frac{1}{2}\{\mathcal{A}^+, \mathcal{A}^-\} = \hat{N} + 3/2$, so

$$H = \frac{1}{2}\{\mathcal{A}^+, \mathcal{A}^-\} + i\frac{v}{\sqrt{2}}(\mathcal{A}^+ - \mathcal{A}^-). \quad (A.51)$$

If we chose $e^{i\Delta\phi} = -1$, we see that the matrix elements for $\mathbf{p}\cdot\boldsymbol{\sigma} = \frac{i}{\sqrt{2}}(\mathcal{A}^+ - \mathcal{A}^-)$ are:

$$\langle n_r', j, m, +|\frac{i}{\sqrt{2}}(\mathcal{A}^+ - \mathcal{A}^-)|n_r, j, m, -\rangle = i(\sqrt{n_r+1}\delta_{n_r+1,n_r'} - \sqrt{n_r+j+1}\delta_{n_r,n_r'}) \quad (A.52)$$

$$\langle n_r', j, m, -|\frac{i}{\sqrt{2}}(\mathcal{A}^+ - \mathcal{A}^-)|n_r, j, m, +\rangle = i(\sqrt{n_r+j+1}\delta_{n_r,n_r'} - \sqrt{n_r}\delta_{n_r-1,n_r'}). \quad (A.53)$$

Appendix B.

In this appendix we calculate the radial Schrödinger equation in position space by Fourier transforming the momentum-space version. We want to find the Fourier transform of the eigenfunctions of the harmonic oscillator. We first need to find the momentum space eigenfunctions of the three-dimensional spherical harmonic oscillator int terms of the momentum space harmonic oscillator wavefunctions $\langle\mathbf{p}|\psi_{nlm}\rangle = \int \frac{d\mathbf{r}}{\sqrt{(2\pi)^3}} e^{i\mathbf{p}\cdot\mathbf{r}}\langle\mathbf{r}|\psi_{nlm}\rangle$. Using the expansion of plane waves into spherical harmonics, $e^{i\mathbf{p}\cdot\mathbf{r}} = 4\pi\sum_{lm} i^l j_l(pr)Y_l^m(\hat{\mathbf{p}})\left(Y_l^m(\hat{\mathbf{r}})\right)^*$, we find the relation

$$\langle\mathbf{p}|\psi_{nlm}\rangle = \int \frac{d\mathbf{r}}{\sqrt{(2\pi)^3}}4\pi \times \sum_{l'm'} i^{l'} j_{l'}(pr)Y_{l'}^{m'}(\hat{\mathbf{p}})\left(Y_{l'}^{m'}(\hat{\mathbf{r}})\right)^*\langle\mathbf{r}|\psi_{nlm}\rangle \quad (B.1)$$

$$= \sqrt{\frac{2}{\pi}} i^l Y_l^m(\hat{\mathbf{p}})\int dr(r^2 j_l(pr)R_{ln}(r)). \quad (B.2)$$

To find the radial Schrödinger's equation for the Weyl coupling in position space,

$$\left[-\frac{\nabla_{\mathbf{p}}^2}{2} + \frac{\mathbf{p}^2}{2} + v\mathbf{p}\cdot\boldsymbol{\sigma}\right]\psi_{njm}(\mathbf{p}) = E_{nj}\psi_{njm}(\mathbf{p}) \quad (B.3)$$

it is easiest to begin with the same equation in momentum space, and Fourier transform the eigenstates $\psi_{njm}(\mathbf{p}) = \int e^{i\mathbf{p}\cdot\mathbf{r}}\phi_{njm}(\mathbf{r})d\mathbf{r}$. But recall, we have showed that j and m are good quantum numbers, and the eigenfunctions have the form $\psi_{njm}(\mathbf{p}) = f_n^+(p)\chi_{jm}^+(\hat{\mathbf{p}}) + f_n^-(p)\chi_{jm}^-(\hat{\mathbf{p}})$. The spinors $\chi_{jm}^\pm$ contain spherical harmonics of order $l = j \mp \frac{1}{2}$, so they are eigenfunctions of the Fourier transform. The position space wavefunction thus has the form

$$\phi_{njm}(\mathbf{r}) = 4\pi\int\frac{d^3\mathbf{r}}{\sqrt{(2\pi)^3}}\left[\sum_{lm}(-i)^l j_l(pr)Y_l^m(\hat{\mathbf{p}})\left(Y_l^m(\hat{\mathbf{r}})\right)^*\right] \times \left(f_n^+(p)\chi_{jm}^+(\hat{\mathbf{p}}) + f_n^-(p)\chi_{jm}^-(\hat{\mathbf{p}})\right) \quad (B.4)$$

$$= \sqrt{\frac{2}{\pi}}(-i)^{j-\frac{1}{2}}\left(-ig_n^+(r)\chi_{jm}^+(\hat{\mathbf{r}}) + g_n^-(r)\chi_{jm}^-(\hat{\mathbf{r}})\right), \quad (B.5)$$

where $g_n^\pm(r) = \int p^2 j_l(pr)f_n^\pm(p)\,dp$, and $l = j \mp \frac{1}{2}$.

We are now ready to transform the momentum-space Schrödinger equation, we first multiply by $e^{i\mathbf{p}\cdot\mathbf{r}}$, and then integrate over momentum to get

$$\int\frac{d^3\mathbf{p}}{\sqrt{(2\pi)^3}}e^{i\mathbf{p}\cdot\mathbf{r}}\left[-\frac{\nabla_{\mathbf{p}}^2}{2} + \frac{\mathbf{p}^2}{2} + v\mathbf{p}\cdot\boldsymbol{\sigma}\right]\psi_{njm}(\mathbf{p}) = E_{nj}\int\frac{d^3\mathbf{p}}{\sqrt{(2\pi)^3}}e^{i\mathbf{p}\cdot\mathbf{r}}\psi_{njm}(\mathbf{p}). \quad (B.6)$$

Transforming this term-by-term, the momentum space kinetic term becomes a position space trapping term

$$\int\frac{d^3\mathbf{p}}{\sqrt{(2\pi)^3}}e^{i\mathbf{p}\cdot\mathbf{r}}\left(\frac{-\nabla_{\mathbf{p}}^2}{2}\right)\psi_{njm}(\mathbf{p}) = \frac{1}{2}\mathbf{r}^2\phi_{njm}(\mathbf{r}), \quad (B.7)$$

Similarly, the momentum space trap becomes a kinetic energy term in position space

$$\int \frac{\mathrm{d}^3\mathbf{p}}{\sqrt{(2\pi)^3}}\left(\frac{\mathbf{p}^2}{2}\right)\mathrm{e}^{\mathrm{i}\mathbf{p}\cdot\mathbf{r}}\psi_{njm}(\mathbf{p})$$
$$= -\frac{\nabla^2}{2}\int \frac{\mathrm{d}^3\mathbf{p}}{\sqrt{(2\pi)^3}}(\psi_{njm}(\mathbf{p})\,\mathrm{e}^{\mathrm{i}\mathbf{p}\cdot\mathbf{r}}) \tag{B.8}$$
$$= -\frac{\nabla^2}{2}\phi_{njm}(\mathbf{r}). \tag{B.9}$$

The spin–orbit term is more complicated, we first use the property that $\mathbf{p}\cdot\boldsymbol{\sigma}\chi^{\pm}_{jm}(\hat{\mathbf{p}}) = p\chi^{\mp}_{jm}(\hat{\mathbf{p}})$

$$\int \frac{\mathrm{d}^3\mathbf{p}}{\sqrt{(2\pi)^3}}[\mathrm{e}^{\mathrm{i}\mathbf{p}\cdot\mathbf{r}}v(\mathbf{p}\cdot\boldsymbol{\sigma})\psi_{njm}(\mathbf{p})] = v\int \frac{\mathrm{d}^3\mathbf{p}}{\sqrt{(2\pi)^3}}$$
$$\times\left[\mathrm{e}^{\mathrm{i}\mathbf{p}\cdot\mathbf{r}}p\big(f^+_n(p)\chi^-_{jm}(\hat{\mathbf{p}}) + f^-_n(p)\chi^+_{jm}(\hat{\mathbf{p}})\big)\right], \tag{B.10}$$

we then expand the exponential $\mathrm{e}^{\mathrm{i}\mathbf{p}\cdot\mathbf{r}}$ in terms of spherical harmonics,

$$\int \frac{\mathrm{d}^3\mathbf{p}}{\sqrt{(2\pi)^3}}[\mathrm{e}^{\mathrm{i}\mathbf{p}\cdot\mathbf{r}}v(\mathbf{p}\cdot\boldsymbol{\sigma})\psi_{njm}(\mathbf{p})]$$
$$= v\frac{4\pi}{\sqrt{(2\pi)^3}}\sum_{lm} i^l\int \mathrm{d}\hat{\mathbf{p}}\int \mathrm{d}p p^3\big[j_l(pr)Y^m_l(\hat{\mathbf{r}})\big(Y^m_l(\hat{\mathbf{p}})\big)^*$$
$$\times\big(f^+_n(p)\chi^-_{jm}(\hat{\mathbf{p}}) + f^-_n(p)\chi^+_{jm}(\hat{\mathbf{p}})\big)\big]$$
$$= v\frac{4\pi}{\sqrt{(2\pi)^3}}i^{j-\frac{1}{2}}\Bigg[\mathrm{i}\int \mathrm{d}p\big(p^3 j_{j+\frac{1}{2}}(pr)f^-_{nj}(p)\big)\chi^+_{jm}(\hat{\mathbf{r}})$$
$$+\int \mathrm{d}p\big(p^3 j_{j-\frac{1}{2}}(pr)f^+_{nj}(p)\big)\chi^-_{jm}(\hat{\mathbf{r}})\Bigg].$$

The spinors $\chi^{\pm}_{jm}$ have angular momentum components $l = j\mp\frac{1}{2}$. These angular momentum variables do not match the angular momentum corresponding to the spinors multiplying them. This, along with the extra factor of p in the integrand $\int \mathrm{d}p(p^3 j_l(pr)f(p)) = \int \mathrm{d}p\, p^2(p j_l(pr)f(p))$, suggest it would be helpful to express the term $p j_{j_{\pm\frac{1}{2}}}(pr)$ in terms of spherical Bessel functions of the order $j\mp\frac{1}{2}$. We use the identities

$$z j_l(z) = z\frac{\mathrm{d}}{\mathrm{d}z}j_{l+1}(z) + (l+2)j_{l+1}(z) \tag{B.11}$$

$$z j_l(z) = -z\frac{\mathrm{d}}{\mathrm{d}z}j_{l-1}(z) + (l-1)j_{l-1}(z) \tag{B.12}$$

to express

$$p j_l(pr) = \left(\frac{\mathrm{d}}{\mathrm{d}r} + \frac{l+2}{r}\right)j_{l+1}(pr) \tag{B.13}$$

$$= \left(-\frac{\mathrm{d}}{\mathrm{d}r} + \frac{l-1}{r}\right)j_{l-1}(pr). \tag{B.14}$$

These relations convert the product $p j_l(pr)$ into a differential operator in r that can be removed from the integral. Together, these give the expression for the Fourier transform of the three-dimensional spin–orbit coupling term

$$\int \frac{\mathrm{d}^3\mathbf{p}}{\sqrt{(2\pi)^3}}[\mathrm{e}^{\mathrm{i}\mathbf{p}\cdot\mathbf{r}}v(\mathbf{p}\cdot\boldsymbol{\sigma})\psi_{njm}(\mathbf{p})] = v\sqrt{\frac{2}{\pi}}i^{j-\frac{1}{2}}$$
$$\times\left[\mathrm{i}\left(-\frac{\mathrm{d}}{\mathrm{d}r} + \frac{j-\frac{1}{2}}{r}\right)\int \mathrm{d}p\big(p^2 j_{j-\frac{1}{2}}(pr)f^-_{nj}(p)\big)\chi^+_{jm}(\hat{\mathbf{r}})\right. \tag{B.15}$$
$$\left.+\left(\frac{\mathrm{d}}{\mathrm{d}r} + \frac{j+\frac{1}{2}}{r}\right)\int \mathrm{d}p\big(p^3 j_{j-\frac{1}{2}}(pr)f^+_{nj}(p)\big)\chi^-_{jm}(\hat{\mathbf{r}})\right] \tag{B.16}$$

$$= v i^{j-\frac{1}{2}}\left[\mathrm{i}\left(-\frac{\mathrm{d}}{\mathrm{d}r} + \frac{j-\frac{1}{2}}{r}\right)g^-_{nj}(r)\chi^+_{jm}(\hat{\mathbf{r}})\right.$$
$$\left.+\left(\frac{\mathrm{d}}{\mathrm{d}r} + \frac{j+\frac{1}{2}}{r}\right)g^+_{nj}(r)\chi^-_{jm}(\hat{\mathbf{r}})\right]. \tag{B.17}$$

Finally, we combine these to get the expression for the radial Schrödinger equation for the three-dimensional spin–orbit coupling in position space,

$$\frac{1}{2}\left[-\frac{1}{r}\left(\frac{\mathrm{d}^2}{\mathrm{d}r^2}r\right) + \frac{\left(j+\frac{1}{2}\right)\left(j+\frac{3}{2}\right)}{r^2} + r^2\right]g^+_{nj}(r)$$
$$+ v\left(-\frac{\mathrm{d}}{\mathrm{d}r} + \frac{j-\frac{1}{2}}{r}\right)g^-_{nj}(r) = E_{nj}g^+_{nj}(r) \tag{B.18}$$

$$\frac{1}{2}\left[-\frac{1}{r}\left(\frac{\mathrm{d}^2}{\mathrm{d}r^2}r\right) + \frac{\left(j+\frac{1}{2}\right)\left(j-\frac{1}{2}\right)}{r^2} + r^2\right]g^-_{nj}(r)$$
$$+ v\left(\frac{\mathrm{d}}{\mathrm{d}r} + \frac{j+\frac{1}{2}}{r}\right)g^+_{nj}(r) = E_{nj}g^-_{nj}(r). \tag{B.19}$$

References

[1] Lin Y J, Compton R L, Jimenez-Garcia K, Porto J V and Spielman I B 2009 *Nature* **462** 628
[2] Lin Y-J, Compton R L, Perry A R, Phillips W D, Porto J V and Spielman I B 2009 *Phys. Rev. Lett.* **102** 130401
[3] Lin Y J, Jimenez-Garcia K and Spielman I B 2011 *Nature* **471** 83
[4] Lin Y-J, Compton R L, Jimenez-Garcia K, Phillips W D, Porto J V and Spielman I B 2011 *Nature Phys.* **7** 531
[5] Aidelsburger M, Atala M, Nascimbène S, Trotzky S, Chen Y-A and Bloch I 2011 *Phys. Rev. Lett.* **107** 255301
[6] Campbell D L, Juzeliūnas G and Spielman I B 2011 *Phys. Rev.* A **84** 025602
[7] Ruseckas J, Juzeliūnas G, Öhberg P and Fleischhauer M 2005 *Phys. Rev. Lett.* **95** 010404
[8] Juzeliūnas G, Ruseckas J and Dalibard J 2010 *Phys. Rev.* A **81** 053403
[9] Dalibard J, Gerbier F, Juzeliūnas G and Öhberg P 2011 *Rev. Mod. Phys.* **83** 1523
[10] Stanescu T D, Anderson B and Galitski V 2008 *Phys. Rev.* A **78** 023616
[11] Stanescu T D, Zhang C and Galitski V 2007 *Phys. Rev. Lett.* **99** 110403
[12] Hu H, Ramachandhran B, Pu H and Liu X-J 2012 *Phys. Rev. Lett.* **108** 010402
[13] Ramachandhran B, Opanchuk B, Liu X-J, Pu H, Drummond P D and Hu H 2012 *Phys. Rev.* A **85** 023606
[14] Sinha S, Nath R and Santos L 2011 *Phys. Rev. Lett.* **107** 270401
[15] Ghosh S K, Vyasanakere J P and Shenoy V B 2011 *Phys. Rev.* A **84** 053629
[16] Li Y, Zhou X and Wu C 2012 *Phys. Rev.* B **85** 125122
[17] Cappelluti E, Grimaldi C and Marsiglio F 2007 *Phys. Rev. Lett.* **98** 167002
[18] Magarill A V Chaplikand L I 2006 *Phys. Rev. Lett.* **96** 126402

[19] Vyasanakereand J P and Shenoy V B 2012 *New J. Phys.* **14** 043041
[20] Cui X 2012 *Phys. Rev.* A **85** 022705
[21] Takei S, Lin C-H, Anderson B M and Galitski V 2012 *Phys. Rev.* A **85** 023626
[22] Vyasanakereand J P and Shenoy V B 2011 *Phys. Rev.* B **83** 094515
[23] Gong M, Tewari S and Zhang C 2011 *Phys. Rev. Lett.* **107** 195303
[24] Zhai Z-Q Yuand H 2011 *Phys. Rev. Lett.* **107** 195305
[25] Vyasanakere J P, Zhang S and Shenoy V B 2011 *Phys. Rev.* B **84** 014512
[26] Barnett R, Powell S, Graß T, Lewenstein M and Das Sarma S 2012 *Phys. Rev.* A **85** 023615
[27] Anderson B M, Juzeliūnas G, Galitski V M and Spielman I B 2012 *Phys. Rev. Lett.* **108** 235301
[28] Bermudez A, Mazza L, Rizzi M, Goldman N, Lewenstein M and Martin-Delgado M A 2010 *Phys. Rev. Lett.* **105** 190404
[29] Wan X, Turner A M, Vishwanath A and Savrasov S Y 2011 *Phys. Rev.* B **83** 205101
[30] Marshalek E R 1992 *J. Math. Phys.* **33** 2972
[31] NIST 2012 *Digital Library of Mathematical Functions* National Institute of Standards and Technology (available at http://dlmf.nist.gov/18.3.T1)
[32] NIST 2012 *Digital Library of Mathematical Functions* National Institute of Standards and Technology (available at http://dlmf.nist.gov/10.47)
[33] Kawakami T, Mizushima T, Nitta M and Machida K 2012 *Phys. Rev. Lett.* **109** 015301
[34] Li Y, Zhou X and Wu C 2012 arXiv:1205.2162 [cond-mat.quant-gas]